Neuropharmacology 67 (2013) 403–411

Contents lists available at SciVerse ScienceDirect

Neuropharmacology

journal homepage: www.elsevier.com/locate/neuropharm

Novel multitarget ligand ITH33/IQM9.21 provides neuroprotection in *in vitro* and *in vivo* models related to brain ischemia

Silvia Lorrio [a,b,f,1], Vanessa Gómez-Rangel [a,b,1], Pilar Negredo [a,3], Javier Egea [a,b,e], Rafael Leon [a,e], Alejandro Romero [a,b,2], Tharine Dal-Cim [g], Mercedes Villarroya [a,b], Maria Isabel Rodriguez-Franco [d], Santiago Conde [d], Mariana P. Arce [d], Jose María Roda [f], Antonio G. García [a,b,c,e], Manuela G. López [a,b,*]

[a] *Instituto Teófilo Hernando, Universidad Autónoma de Madrid, Madrid, Spain*
[b] *Departamento de Farmacología y Terapéutica, Facultad de Medicina, Universidad Autónoma de Madrid, Madrid, Spain*
[c] *Servicio de Farmacología Clínica, Instituto de Investigación Sanitaria, Hospital la Princesa, Universidad Autónoma de Madrid, Spain*
[d] *Instituto de Química Médica, Consejo Superior de Investigaciones Científicas (IQM-CSIC), Madrid, Spain*
[e] *Instituto de Investigación Sanitaria, Hospital Universitario la Princesa, Universidad Autónoma de Madrid, Spain*
[f] *Instituto de Investigación Sanitaria IdiPAZ, Hospital Universitario la Paz, Universidad Autónoma de Madrid, Spain*
[g] *Departamento de Bioquímica, Universidade Federal de Santa Catarina, Florianópolis, Brazil*

ARTICLE INFO

Article history:
Received 24 August 2012
Received in revised form
27 November 2012
Accepted 3 December 2012

Keywords:
Neuroprotection
ITH33/IQM9.21
Oxygen and glucose deprivation
Photothrombotic stroke
Free radicals
Hippocampal slices
iNOS
GSH

ABSTRACT

ITH33/IQM9.21 is a novel compound belonging to a family of glutamic acid derivatives, synthesized under the hypothesis implying that multitarget ligands may provide more efficient neuroprotection than single-targeted compounds. In rat hippocampal slices, oxygen plus glucose deprivation followed by re-oxygenation (OGD/Reox) elicited 42% cell death. At 1 μM, ITH33/IQM9.21 mitigated this damage by 26% and by 55% at 3 μM. OGD/Reox also elicited mitochondrial depolarization, overproduction of reactive oxygen species (ROS), enhanced expression of nitric oxide synthase (iNOS) and reduction of GSH levels. These changes were almost fully prevented when 3 μM ITH33/IQM9.21 was present during slice treatment with OGD/Reox. In isolated hippocampal neurons, ITH33/IQM9.21 reduced $[Ca^{2+}]_c$ transients induced by a high K^+ depolarizing solution or glutamate. In a photothrombotic model of stroke in mice, intraperitoneal injection of ITH33/IQM9.21 at 1.25 mg/kg, 2.5 mg/kg or 5 mg/kg given before and during 2 days after stroke induction, reduced infarct volume by over 45%. Furthermore, when the compound was administered 1 h post-stroke, a similar effect was observed. In conclusion, these *in vitro* and *in vivo* results suggest that ITH33/IQM9.21 exhibits neuroprotective effects to protect the vulnerable neurons at the ischemic penumbra by an effective and multifaceted mechanism, mediated by reduction of Ca^{2+} overload, providing mitochondrial protection and antioxidant actions.

1. Introduction

During the last 30 years, about 50 compounds that showed neuroprotection in *in vitro* and *in vivo* animal models of stroke have provided disappointing negative outcomes in clinical trials. The causes for such failure were analyzed by an international committee that elaborated a careful report suggesting the actions to be taken in order to optimize the preclinical studies in *in vitro*, but particularly in *in vivo* models of cerebral ischemia to ensure a more successful translation to the clinic of preclinical results (Fisher et al., 2005). However, after nearly 7 years since the STAIR criteria were established, clinical trials continue to provide negative outcomes. The example of the antioxidant NXY-059 illustrates this problem since it produced positive outcomes in the first clinical trial (Lees et al., 2006) but a second study with a greater sample of patients gave negative results (Shuaib et al., 2007). Thus, novel strategies should be approached in searching compounds with neuroprotective actions in stroke.

The multitarget ligand (MTL) hypothesis implies that a compound targeting two or more signaling pathways leading to apoptotic death of vulnerable neurons, should be more effective than a single target ligand targeting only one of those pathways

* Corresponding author. Instituto Teófilo Hernando, Departamento de Farmacología, Facultad de Medicina, Universidad Autónoma de Madrid, C/Arzobispo Morcillo 4, E-28029 Madrid, Spain. Tel.: +34 914975386; fax: +34 914973120.
E-mail address: manuela.garcia@uam.es (M.G. López).
[1] Equal contributors.
[2] Present address: Departamento de Toxicología y Farmacia, Facultad de Veterinaria, Universidad Complutense de Madrid, 28040 Madrid, Spain.
[3] Present address: Departamento de Anatomía, Histología y Neurociencia, Facultad de Medicina, Universidad Autónoma de Madrid, Madrid, Spain.

0028-3908/$ – see front matter © 2012 Elsevier Ltd. All rights reserved.
http://dx.doi.org/10.1016/j.neuropharm.2012.12.001

(Leon et al., 2013). In the frame of this hypothesis we recently designed and synthesized a new family of MTLs taking L-glutamic acid as a suitable biocompatible linker to join three pharmacophoric groups: (1) an ω-situated *N*-benzylpiperidine moiety to inhibit acetylcholinesterase (AChE) by interacting with its catalytic active site; (2) an N-protecting group of the amino acid, capable of interacting with the peripheral site of AChE that is known to be linked to aggregation of amyloid beta (Aβ) to form oligomers and fibrils (Alvarez et al., 1997) and having as well antioxidant properties; and (3) a lipophilic alkyl ester that could facilitate the crossing of the blood brain barrier. Its molecular structure (*N*-benzoyl-L-GLu [NH-2-(1-benzylpiperidin-4-yl)ethyl]-*O*-nHex) is shown in Fig. 1. Several members of this family exhibited these expected properties, as well as *in vitro* neuroprotection against oxidative stress in human neuroblastoma SH-SY5Y cells (Arce et al., 2009). Compound ITH33/IQM9.21 was selected from this family for further testing in different *in vitro* and *in vivo* models of neurons made vulnerable with different kinds of stress stimuli.

The hypothesis that this profile could make ITH33/IQM9.21 a suitable compound for neuroprotection in stroke was formulated on the basis of the following observations: (1) AChE inhibitors have shown neuroprotection on *in vitro* models of excitotoxicity, free radicals, Ca^{2+} overload (Arias et al., 2005; Takada-Takatori et al., 2006), and oxygen and glucose deprivation (OGD) (Akasofu et al., 2003; Sobrado et al., 2004) as well as in *in vivo* models of stroke (Fujiki et al., 2005; Lorrio et al., 2007), implying that enhanced cholinergic neurotransmission could provide neuroprotection under cerebral ischemic conditions; (2) the link between certain pathogenic mechanisms of Alzheimer's disease (AD) and cerebrovascular disease has been illustrated, for instance in rodents exposed to ischemia, Aβ production is augmented (Garcia-Alloza et al., 2011) and hyperphosphorylated tau is observed in cortical neurons (Gordon-Krajcer et al., 2007), (3) ITH33/IQM9.21 affords neuroprotection against oxidative stress *in vitro* (Arce et al., 2009); and (4) ITH33/IQM9.21 blocks voltage-dependent Ca^{2+} currents and reduces the transient elevations of cytosolic Ca^{2+} concentrations elicited by depolarizing stimuli (Maroto et al., 2011).

In this context, it seemed appropriate to investigate whether compound ITH33/IQM9.21 could also exert neuroprotection in *in vitro* and *in vivo* models of cerebral ischemia. We demonstrate here that ITH33/IQM9.21 provides neuroprotection of rat hippocampal slices subjected to OGD followed by re-oxygenation; such effect was associated to reduction of mitochondrial depolarization, decreased generation of reactive oxygen species (ROS) and inducible nitric oxide synthase (iNOS) and restoration of glutathione (GSH) levels. Furthermore, in isolated rat hippocampal neurons ITH33/IQM9.21 reduced intracellular Ca^{2+} transients induced by glutamate or depolarization caused by high potassium. Finally, ITH33/IQM9.21 diminished the volume of cortical infarct in a mouse model of photothrombotic stroke not only when administered before, but also when given 1 h post-induction of stroke.

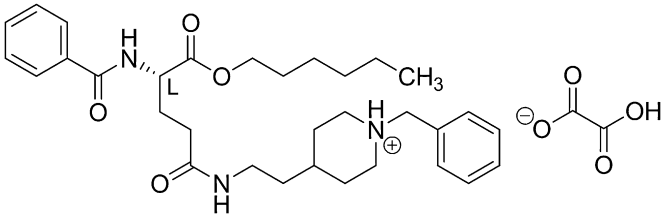

Fig. 1. Chemical structure of compound ITH33/IQM9.21 (*N*-benzoyl-L-Glu[*NH*-2-(1-benzylpiperidin-4-yl)ethyl]-*O*-nHex).

2. Materials and methods

2.1. Materials

Melatonin was from Sigma (Madrid, Spain). Chemicals to prepare different nutrient solutions were chemical grade from Panreac (Madrid Spain). Compound ITH33/IQM9.21 was synthesized as described by Arce et al. (2009).

2.2. Use of animals

All experimental procedures were performed following the *Guide for the Care and Use of Laboratory Animals* and were previously approved by the institutional Ethics Committee of the Universidad Autónoma de Madrid, Spain, according to the European Guidelines for the use and care of animals for research in accordance with the European Communities Council Directive of 24 November 1986 (86/609/EEC) and with the Spanish Real Decreto of 10 October 2005 (RD 1201/2005). All efforts were made to minimize animal suffering and to reduce the number of animals used.

2.3. Preparation of rat hippocampal slices and induction of oxygen and glucose deprivation followed by re-oxygenation (OGD/Reox)

Adult male Sprague–Dawley rats (275–325 g) from a colony of our animal quarters were used. *In vitro* damage caused by OGD/Reox and the protection elicited by ITH33/IQM9.21 was studied in acutely isolated rat hippocampal slices. The protocol was similar to that previously described by Egea and co-workers (Egea et al., 2007; Maroto et al., 2011). Rats were quickly decapitated under sodium pentobarbital anesthesia (60 mg/kg, i.p.), forebrains were rapidly removed from the skull and placed into ice-cold Krebs bicarbonate dissection buffer (pH 7.4), containing (in mM): NaCl 120, KCl 2, $CaCl_2$ 0.5, $NaHCO_3$ 26, $MgSO_4$ 10, KH_2PO_4 1.18, glucose 11 and sucrose 200. The chamber solutions were pre-bubbled with either 95% O_2/5% CO_2 or 95% N_2/5% CO_2 gas mixtures, for at least 45 min before slice immersion, to ensure O_2 saturation or removal. The hippocampi were quickly dissected, and slices (350 μm thick) were rapidly prepared using a McIlwain Tissue Chopper. Then, the slices were transferred to vials of sucrose-free dissection buffer, bubbled with 95% O_2/5% CO_2 in a water bath at room temperature for 60 min, to allow tissue recovery from slicing trauma before starting the experiments (equilibration period). The slices corresponding to the control group were incubated 15 min in a Krebs solution with the following composition (in mM): NaCl 120, KCl 2, $CaCl_2$ 2, $NaHCO_3$ 26, $MgSO_4$ 1.19, KH_2PO_4 1.18 and glucose 11; this solution was equilibrated with 95% O_2/5% CO_2. Oxygen and glucose deprivation was induced by incubating the slices for a 15 min period in a glucose-free Krebs solution, equilibrated with a 95% N_2/5% CO_2 gas mixture; glucose was replaced by 2-deoxyglucose. After this OGD period, the slices were returned back to an oxygenated normal Krebs solution containing glucose (re-oxygenation period). Experiments were performed at 37 °C. A control and an OGD group were included in all experiments and four drug concentrations were tested in each experiment. When treated, OGD slices received ITH33/IQM9.21 and remained there during the OGD and re-oxygenation period (see Fig. 2A for experimental protocol).

2.4. Quantification of viability by MTT in hippocampal slices

Hippocampal cell viability was determined through the ability of the cells to reduce MTT (Denizot and Lang, 1986). Hippocampal slices were collected immediately after the re-oxygenation period and were incubated with MTT (0.5 mg/ml) in Krebs bicarbonate solution for 30 min at 37 °C. The tetrazolium ring of MTT can be cleaved by active dehydrogenases in order to produce a precipitated formazan derivative. The formazan produced was solubilized by adding 200 μl DMSO, resulting in a colored compound whose optical density was measured spectrophotometrically at 540 nm using a microplate reader (Labsystems iEMS reader MF; Labsystems, Helsinki, Finland). Absorbance values obtained in control slices were taken as 100% viability.

2.5. Measurement of ROS production in hippocampal slices

To measure the generation of reactive oxygen species (ROS), we have used the molecular probe H_2DCFDA (Ha et al., 1997) which diffuses through the cell membrane and is hydrolyzed by intracellular esterases to the non-fluorescent form dichlorofluorescein (DCFH). DCFH reacts with intracellular H_2O_2 to form dichlorofluorescin (DCF), a green fluorescent dye. Immediately after McIlwain Tissue Chopper sectioning 200 μm thick hippocampal slices were loaded with 80 μM H_2DCFDA for 45 min in Krebs solution. Subsequently, slices were washed twice with Krebs solution and kept for 15 min before the beginning of the experiment. Fluorescence was measured in a fluorescence inverted NIKON eclipse T2000-U microscope. Wavelengths of excitation and emission were 485 and 520 nm, respectively. Images were taken at CA1 at magnifications of 100×. Fluorescence analysis was performed using the Metamorph programme version 7.0. Fluorescence in basal conditions was taken as 1 and experimental variables were normalized with respect to this value.

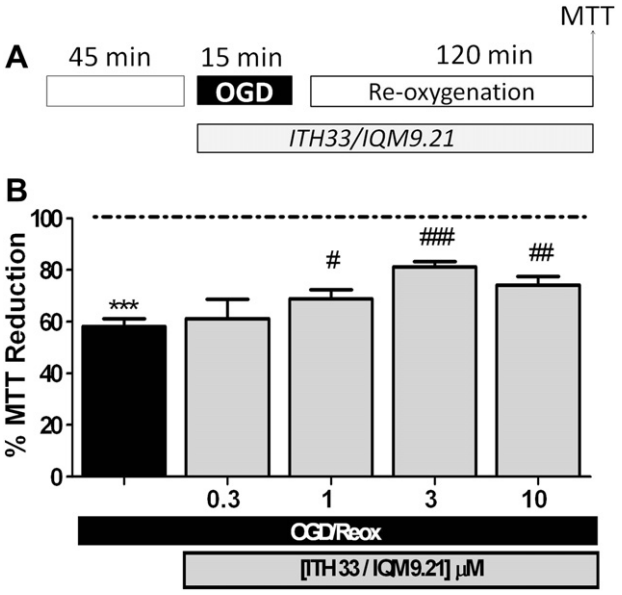

Fig. 2. ITH33/IQM9.21 increases cell viability of rat hippocampal slices subjected to OGD/Reox. (A) Experimental protocol. ITH33/IQM9.21 was introduced in the bathing solution at increasing concentrations during the 15 min OGD period and during the 120 min re-oxygenation period; at the end of the experiment, viability was assessed by measuring MTT reduction. (B) Pooled data corresponding to the mean and S.E.M. of 5 independent experiments. $^{***}p < 0.001$ respect basal slices (not exposed to OGD/Reox) and $^{\#}p < 0.05$, $^{\#\#}p < 0.01$ and $^{\#\#\#}p < 0.001$ respect to slices subjected to OGD/Reox in the absence of neuroprotective compounds.

2.6. Western blot analysis of iNOS

At the end of the experiments slices of each group were lysed in 100 μl ice-cold lysis buffer (1% Nonidet P-40, 10% glycerol, 137 mM NaCl, 20 mM Tris–HCl, pH 7.5, 1 μg/ml leupeptin, 1 mM phenylmethylsulfonyl fluoride, 20 mM NaF, 1 mM sodium pyrophosphate, and 1 mM Na_3VO_4). A tablet of protease inhibitor cocktail (complete Mini, Roche) was added for each 10 ml of buffer A. Protein (30 μg) from these lysates were resolved by SDS–PAGE and transferred to Immobilon-P membranes (Millipore Corp.). Membranes were incubated with anti-iNOS (1:1000). Appropriate peroxidase-conjugated secondary antibodies (1:10,000) were used to detect proteins by enhanced chemiluminescence. Optical density was quantified using the program Scion Image® Alpha 4.0.3.2. Control conditions were taken as 100% and experimental variables were normalized with respect to this value.

2.7. Intracellular GSH measurement

To quantify free GSH we used monochlorobimane, a fluorescent dye that is not fluorescent itself until it reacts with GSH to form a highly fluorescent adduct (Fernandez-Checa and Kaplowitz, 1990) mediated by glutathione S-transferase (Kamencic et al., 2000). Hippocampal slices were suspended in 50 μL potassium phosphate buffer (100 mM, pH 7.4) and mechanically disaggregated by sonication (3–10 s, power 2) in ice. The reaction started by the addition of monochlorobimane (100 μM) and glutathione S-transferase (0.5 U/ml) in a final volume of 100 μl of potassium phosphate buffer (100 mM, pH 7.4). The reaction was monitored in a FLUOstar Optima microplate reader (BMG technologies, Germany) at excitation and emission wavelengths of 410 and 485 nm respectively over 1 h at room temperature. All measurements were done in triplicate in three different hippocampal slices. In the absence of glutathione S-transferase, the rate of adduct formation was very slow; therefore, the use of glutathione S-transferase eliminates the interference of free thiol groups present in other proteins due to its high selectivity for GSH.

2.8. Estimation of mitochondrial membrane potential (Ψ) with TMRE in hippocampal slices

Tetramethylrhodamine ethyl ester (TMRE) is a cationic lipophilic dye that accumulates in the negatively charged mitochondrial matrix according to the Nernst equation potential (Ehrenberg et al., 1988). A TMRE (Molecular Probes, Leiden, The Netherlands) stock solution was prepared at a concentration of 10 mg/ml in DMSO and stored at 0 °C. Working stocks of 1 mg/ml were made up in fresh in distilled water. For estimation of Ψ, at the end of the experiment hippocampal slices were loaded with 100 nM TMRE for 15 min at room temperature in Krebs solution. Fluorescence was measured in a fluorescence inverted NIKON eclipse T2000-U microscope coupled to a digital CCD camera Hamamatsu ORCA-ER. Wavelengths of excitation and emission were 450 and 580 nm, respectively. Images were taken at CA1 at magnifications of 100×. Fluorescence analysis was performed using the Metamorph program version 7.0. Fluorescence in basal conditions was taken as 1 and experimental variables were normalized with respect to this value.

2.9. Isolation and culture of rat hippocampal neurons

Experiments to study changes of the $[Ca^{2+}]_c$ were performed in primary cultures of hippocampal neurons that were prepared from 18-day old rat embryos. After decapitation, the hippocampi were dissected under a stereomicroscope in phosphate-buffered saline at 4 °C. The tissue was digested with 0.5 mg/mL papain and 0.25 mg/mL DNAase dissolved in Ca^{2+}- and Mg^{2+}-free phosphate-buffered saline containing 1 mg/mL bovine serum albumin and 6 mM glucose at 37 °C for 20 min. The papain solution was replaced by 5 mL of Neurobasal medium supplemented with 10% fetal bovine serum. The digested tissue was disaggregated and the cell suspension centrifuged for 4 min at 120 g. Cells were resuspended in 5 mL Neurobasal medium and plated at a desired density on plates coated with poly-D-lysine (0.1 mg/mL). Cells were plated in Neurobasal medium supplemented with 10% fetal bovine serum, 50 μg/mL streptomycin–penicillin and 50 μg/mL gentamicin, and maintained in an incubator at 37 °C with 5% CO_2. After 4 h, the medium was replaced by fresh serum-free medium containing B27 supplement, essential for hippocampal neuronal survival. Under these conditions, standard cell survival was 4 weeks; the experiments were performed on neurons after 7–14 days in culture.

2.10. Measurement of intracellular calcium in populations of rat hippocampal neurons

Rat hippocampal neurons were plated in black, bottom transparent 96 well plates coated with poly-D-lysine (0.1 mg/mL) at a density of 35,000 cells per well. Cells were loaded with 3 μM Fluo-4/AM for 1 h at 37 °C in Neurobasal. Then, cells were washed twice with Krebs-HEPES solution containing the following composition (in mM): 140 NaCl, 5.6 KCl, 1.2 $MgCl_2$, 2 $CaCl_2$, 10 HEPES, 11 D-glucose, pH 7.4 and kept at room temperature for 15 min before the beginning of the experiment. ITH33/IQM9.21 was incubated 15 min before injecting concentrated solutions of glutamate (to obtain a final concentration of 100 μM) or potassium (to obtain a final concentration of 70 mM). Fluorescence measurements were carried out for 14 s since the agonists were injected in a microplate reader (FLUOstar Optima, BMG, Germany). Wavelengths of excitation and emission were 485 and 520 nm, respectively. At the end of the experiment, 50 μl of triton 5% was added to each well to calculate maximum fluorescence (F_{max}) and then 50 μl of $MnCl_2$ 1 M to obtain the minimum fluorescence (F_{min}). Drug-evoked responses were expressed as percentage of the fluorescence values at each time point (F) minus minimum fluorescence values (F_0) divided by F_{max}–F_{min} as follows:

$$F_{520} = (F - F_0)/(F_{max} - F_{min})\%$$

The maximum value of F_{520}, obtained for each experiment, was considered as the Peak F_{520} value.

2.11. Induction of focal ischemia in mice

Adult male Swiss mice (12–14 weeks old, weighing 35–40 g; Charles River, Wilmington, MA, USA) were used. Mice were housed individually under controlled temperature and lighting conditions with food and water provided *ad libitum*.

To induce ischemia, animals were anesthetized with 1.5% isoflurane in oxygen under spontaneous respiration. Mice were then placed in a stereotaxic frame (David Kopf Instruments, Tujunga, CA, USA) and body temperature was maintained at 37 ± 0.5 °C using a servo-controlled rectal probe heating pad (Cibertec, Madrid, Spain). A midline scalp incision was made, the skull was exposed with removal of the periosteum, and both Bregma and lambda points were identified. A cold-light (Zeiss KL 1500 LCD, Jena, Germany) was centered using a micromanipulator at 2.0 mm posterior and 3.0 mm lateral to Bregma on the right side using a fiber optic bundle of 1.9 mm in diameter. One milligram (0.1 ml) of the photosensitive dye Rose Bengal (Sigma–Aldrich, St. Louis, MO, USA) dissolved in sterile saline was injected i.p. and 20 min later the brains were illuminated through the intact skull for 30 min. After completion of the surgical procedures, the incision was sutured and the mice were allowed to recover. Animals showed no visible neurological or behavioral damage.

Mice were randomly divided into six groups ($n = 8$), subjected to ischemia and treated as follows: 0.9% NaCl sterile saline solution (ischemia group); 1.25 mg/kg ITH33/IQM9.21 (1.25 group); 2.5 mg/kg ITH33/IQM9.21 (2.5 group); 5 mg/kg ITH33/IQM9.21 (5 group); 10 mg/kg ITH33/IQM9.21 (10 group) and 15 mg/kg melatonin (melatonin group). ITH33/IQM9.21 was dissolved in saline and given i.p. 1 h before the onset of ischemia and twice a day thereafter (see protocol on top part of Fig. 6). Doses were chosen according to previous *in vitro* data. Melatonin was used as a positive control, and it was dissolved in saline with 5% DMSO and administered by i.p. injection 30 min before the onset of ischemia, 24 and 48 h after ischemia, as previously described (Zou et al., 2006).

In the post-stroke administration protocol, two experimental groups were used: the ischemia group and the 5 mg/kg ITH33/IQM9.21. In these animals saline or

compound was administered 1 h post-illumination (Fig. 7); thereafter the administration protocol was the same as that one used in the pre-treatment protocol.

Three days after ischemia, mice were decapitated under deep isoflurane anesthesia. Brains were extracted and freshly cut using acrylic brain matrices (Stoelting Co., Wood Dale, IL, USA) into 8 coronal 1 mm-thick slices. The slices were then stained with 2% 2,3,5-triphenyltetrazolium chloride (TTC) (Panreac, Castellar del Vallés, Spain) in 0.1 M phosphate buffer, pH 7.4, for 30 min at 37 °C and then fixed with freshly prepared 4% paraformaldehyde in 0.1 M phosphate buffer. Both rostral and caudal sides of the slices were digitized and cortical infarct volume was assessed by an observer blinded to the experimental groups using Image J (National Institutes of Health, Bethesda, MD, USA). Briefly, after image calibration, ipsilateral cortex, contralateral cortex and cortical infarct borders were delineated to obtain the areas; volumes were then calculated and the edema's effect was corrected. After addition of the corrected infarct volumes of the 8 slices, and doing the same with the edema, results were expressed as percentage of the ratio relative to the contralateral cortex in order to correct for normal size differences between animals. Finally, the mean of rostral and caudal sides was calculated for each animal.

2.12. Statistical analysis

Results were expressed as mean ± S.D. Statistical differences were determined with ANOVA test followed by Bonferroni *post hoc* using GraphPad Prism 5.00. Statistical significance was set at $p < 0.05$.

3. Results

3.1. Effects of ITH33/IQM9.21 on cell viability of rat hippocampal slices subjected to OGD followed by re-oxygenation

The potential neuroprotective effect of ITH33/IQM9.21 was first studied on an *in vitro* model of cerebral ischemia namely, rat hippocampal slices subjected to a 15 min OGD period followed by a 2 h period of re-oxygenation (OGD/Reox) (Fig. 2A). Cell viability, normalized to 100% of control slices, was reduced by 42% after OGD/Reox (black column in Fig. 2). Incubation of ITH33/IQM9.21 during OGD/Reox reduced cell damage in a concentration-dependent manner; significant protection was obtained at 1 μM (26%) and was maximum at 3 μM (55%) (Fig. 2B).

3.2. Effects of ITH33/IQM9.21 on ROS production and iNOS induction in rat hippocampal slices subjected to OGD/Reox

Because oxidative stress is implicated in the pathogenesis of brain ischemia (Crack and Taylor, 2005; Moro et al., 2004), we tested whether ITH33/IQM9.21 could mitigate such process. The fluorescent probe H_2DCFDA was used to determine the production of ROS under basal conditions, OGD/Reox and after OGD/Reox exposure in the presence of ITH33/IQM9.21. Panels A, B and C of Fig. 3 show illustrative examples of fluorescence in CA1 produced in three slices subjected to the treatments mentioned above. Note that the fluorescence was substantially higher in the OGD/Reox slice, compared with the basal slice; also that the fluorescence of the ITH33/IQM9.21-treated slice and subjected to OGD/Reox was quite close to basal. Furthermore, it can be observed that the pyramidal neuron layer was nearly fully erased in the OGD/Reox slice (Fig. 3B) and that it was preserved (as in the basal condition) in the slice treated with ITH33/IQM9.21 (Fig. 3C). Averaged results are shown in Fig. 3D, showing that OGD/Reox elicited 2.5-fold augmentation of ROS production with respect to control slices (basal); this increase was reduced to 1.2-fold in the slices stressed with OGD/Reox but in the presence of ITH33/IQM9.21.

Since NO overproduction elicited by de novo expression of iNOS also contributes to brain damage (Brown, 2010; Mander et al., 2005; Moro et al., 2004), we explored whether OGD/Reox also caused augmented expression of this enzyme in hippocampal slices. Fig. 3E shows examples of western bands for iNOS and β-actin, obtained from slices that were subjected to the three usual experimental conditions. Note the substantially higher density of iNOS after OGD/Reox, compared with basal; when OGD/Reox was performed in the presence of 3 μM, iNOS increase was close to basal. Averaged results

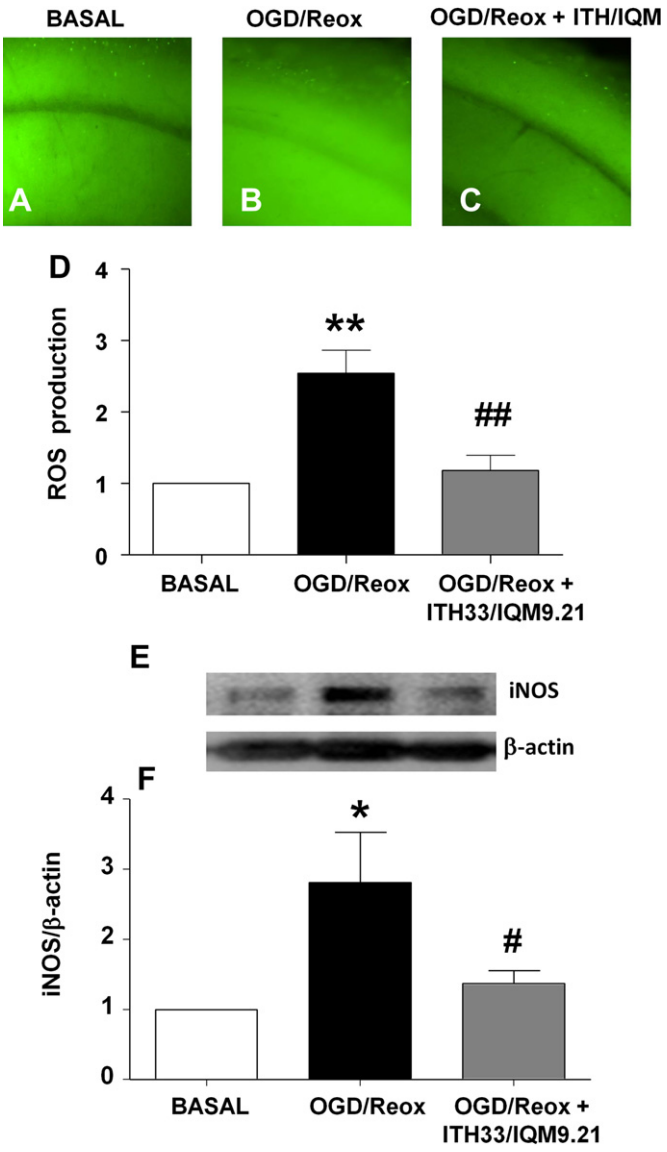

Fig. 3. Compound ITH33/IQM9.21 reduces ROS production and reduces iNOS induction in hippocampal slices elicited by OGD/Reox. The top part figure illustrates DCFDA fluorescence microphotographs of CA1 of hippocampal slices under basal conditions (A), after exposure to OGD/Reox alone (B), or after exposure to OGD/Reox in the presence of 3 μM ITH33/IQM9.21 (C). (D) Average mean data and S.E.M. of 5 independent experiments done with the protocol as in panels A, B and C. $^{**}p < 0.01$ with respect to basal and $^{\#\#}p < 0.01$ in comparison to OGD/Reox alone. (E) Western blot performed on slices following the same protocol of OGD/Reox showing the expression of iNOS and β-actin obtained from protein extracts of slices under basal conditions, exposed to OGD/Reox alone or in the presence of 3 μM ITH33/IQM9.21. (F) Mean and S.E.M. of 5 independent experiments. $^{*}p < 0.05$ with respect to basal and $^{\#}p < 0.05$ in comparison to OGD/Reox alone.

of experiments performed under these three conditions are shown in Fig. 3F; it was observed that iNOS expression was enhanced by 2.8 ± 0.7 fold above basal after OGD/Reox, and such increase was only 1.37 ± 0.2 fold with respect to basal when ITH33/IQM9.21 was present during the OGD/Reox treatment.

3.3. Effects of ITH33/IQM9.21 on GSH levels in hippocampal slices subjected to OGD/Reox

GSH is the most abundant cellular non-thiol protein, playing a central role in maintaining cellular redox status and protecting against oxidative damage (Aoyama et al., 2008). We measured GSH levels in hippocampal slices subjected to 15 min OGD followed by

2 h re-oxygenation. As shown in Fig. 4A, cellular GSH decreased by 36% in hippocampal slices subjected to OGD/Reox respect to control hippocampal slices. Interestingly, application of compound ITH33/IQM9.21 at the concentration of 3 μM during the OGD/Reox period prevented such reduction in GSH levels.

3.4. Effects of ITH33/IQM9.21 on the mitochondrial membrane potential in slices subjected to OGD/Reox

Alteration of mitochondrial function is central stage in the activation of apoptosis and death of vulnerable neurons in stroke. A good indicator of such function is the mitochondrial membrane potential since mitochondria depolarization is a key factor preceding cell death under ischemic conditions (Iijima, 2006). Thus, we thought of interest to study whether ITH33/IQM9.21 affected mitochondrial depolarization in hippocampal slices subjected to OGD/Reox.

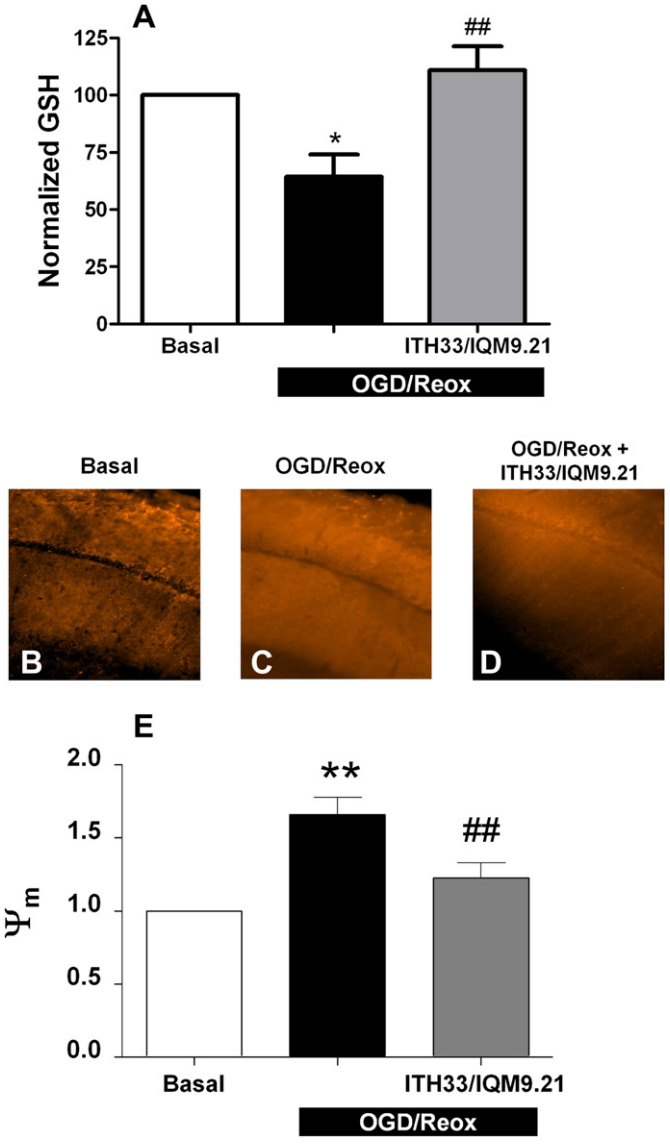

Fig. 4. Compound ITH33/IQM9.21 prevents GSH depletion and reduces mitochondrial depolarization of hippocampal slices subjected to OGD/Reox. (A) Three groups of hippocampal slices were run in parallel: A control group unexposed to OGD/Reox, a group exposed to OGD/Reox alone and a third group exposed to OGD/Reox in the presence of 3 μM of ITH33/IQM9.21. The graph corresponds to the mean and S.E.M. of 4 independent experiments. $^{*}p < 0.05$ respect control slices (not exposed to OGD/Reox) and $^{\#\#}p < 0.01$ respect to slices subjected to OGD/Reox in the absence of ITH33/IQM9.21. Below, TMRE fluorescence microphotographs of area CA1 of hippocampal slices under basal conditions (B), exposed to OGD/Reox alone (C) (OGD/Reox) or in a slice incubated with 3 μM ITH33/IQM9.21 during OGD/Reox (D). (E) Mean and S.E.M. of 5 independent experiments performed with protocols identical to those shown in B, C and D. $^{**}p < 0.01$ with respect to basal and $^{\#\#}p < 0.01$ in comparison to OGD/Reox alone.

Fig. 4B shows a microphotograph of TMRE fluorescence in the hippocampal CA1 area of a non-stressed slice. Fluorescence was enhanced after OGD/Reox treatment, an indication of membrane depolarization (Fig. 4C). In the slice incubated with 3 μM ITH33/IQM9.21, the fluorescence was similar to basal (Fig. 4D). Normalized average data are presented in Fig. 4E. After OGD/Reox, the relative TMRE fluorescence augmented by 1.7-fold with respect to basal, a value that was reduced to 1.2-fold in the presence of ITH33/IQM9.21.

3.5. Effects of ITH33/IQM9.21 on glutamate and potassium-induced $[Ca^{2+}]_c$ elevation in hippocampal neurons

Glutamate excitotoxicity and calcium entry through voltage-dependent calcium channels participate in the ischemic cascade that leads to neuronal cell death (Choi, 1985; Randall and Thayer, 1992). Since ITH33/IQM9.21 blocks VDCCs (Maroto et al., 2011), we thought interesting to explore its effects on glutamate and potassium-induced increases in $[Ca^{2+}]_c$ in fluo-4 loaded rat hippocampal neurons. Glutamate stimulation (100 μM) induced $[Ca^{2+}]_c$ rise of approximately 30% (Fig. 5A); at 3 μM, ITH33/IQM9.21 reduced by 19% the glutamate response (Fig. 5B). As positive control we used the selective NMDA receptor antagonist MK801 at the concentration of 1 μM. MK801 reduced the glutamate induced signal by 31%, being more efficient than ITH33/IQM9.21 to antagonize this parameter (Fig. 5B).

ITH33/IQM9.21 has been described as an antagonist of voltage-dependent calcium channels (Maroto et al., 2011). To evaluate its potential in reducing the calcium entry in hippocampal neurons, we studied the blockade of the signal induced by depolarization with 70 mM K^+. As control we used the unspecific VDCC blocker Cd^{2+} (100 μM). When hippocampal neurons were challenged with a solution containing 70 mM K^+, a transient $[Ca^{2+}]_c$ signal was recorded as an increase in fluorescence intensity. Potassium depolarization induced a maximum signal increase of 45% (Fig. 5C). Positive control Cd^{2+} reduced, almost completely, the calcium increase induced by potassium and only a residual signal of 4% could be detected (Fig. 5C). Under these experimental conditions, ITH33/IQM9.21 was able to block the potassium-induced signal by 38% (Fig. 5D) in a statistically significant manner.

3.6. Effects of ITH33/IQM9.21 on cortical infarct volume in a photothrombotic model of stroke in mice

The positive outcomes on neuroprotection by ITH33/IQM9.21 on an *in vitro* slice model of brain ischemia, gave rise to the relevant question of whether such an effect was also tenable on an *in vivo* model. To answer this question we used a model of focal cortical infarct elicited by permanent occlusion of small vessels by photothrombosis in the mouse (Zou et al., 2006). We used an initial protocol (top part of Fig. 6) that included 5 i.p. injections of ITH33/IQM9.21 (dissolved in saline), 1 before ischemia and 2 doses per day, at days 1 and 2 post-ischemia. Administration of a dose before induction of ischemia was done to ensure the presence of the compound in the blood stream before exposing the animal to stroke and, presumably, optimize protection.

No variations in physiological parameters monitored during the experiments or weight losses were produced. Neither, visible alterations in neurological behavioral parameters were seen.

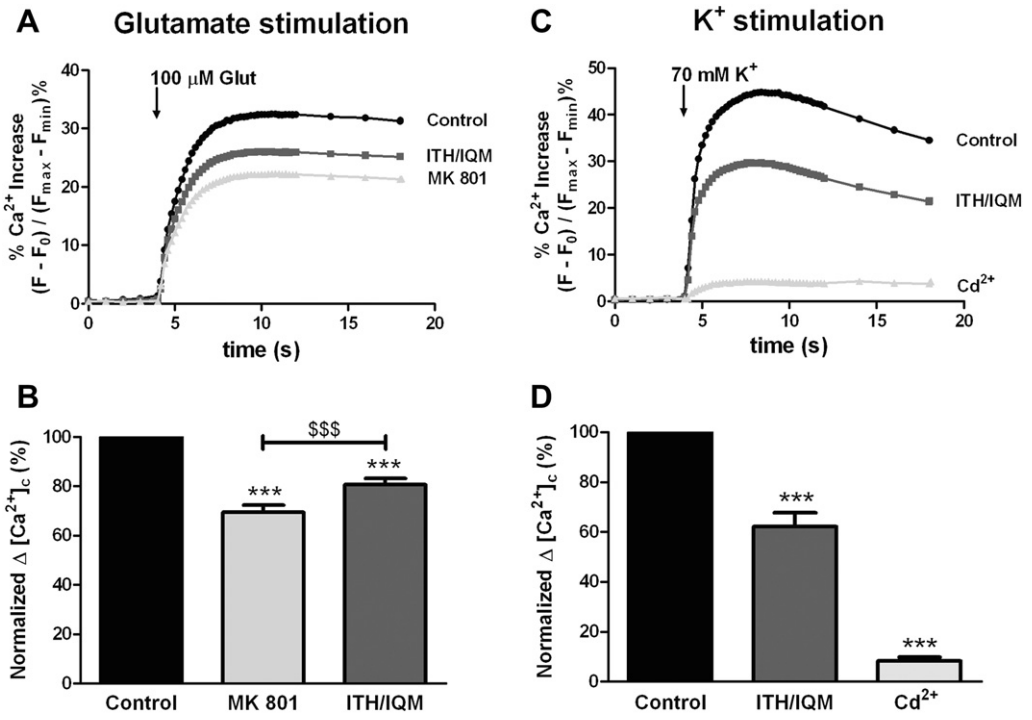

Fig. 5. Blockade by ITH33/IQM9.21 of the $[Ca^{2+}]_c$ elevations in rat hippocampal neurons challenged with glutamate or potassium. Elevations of $[Ca^{2+}]_c$ were elicited in cell populations loaded with Fluo-4. A, C, example records of $[Ca^{2+}]_c$ elevations (ordinates, in % of maximum peak fluorescence) under control conditions or in the presence of 3 μM ITH33/IQM9.21, 1 μM MK801 or 100 μM Cd. B, D, pooled normalized results (% of net $[Ca^{2+}]_c$ increments) from experiments done with protocols A,C. Data are means and S.E.M of 4 different cell cultures; each experiment was performed in triplicate. $^{***}p < 0.001$ compared to control, $^{\$\$\$}p < 0.001$ comparing MK801 and ITH33/IQM9.21.

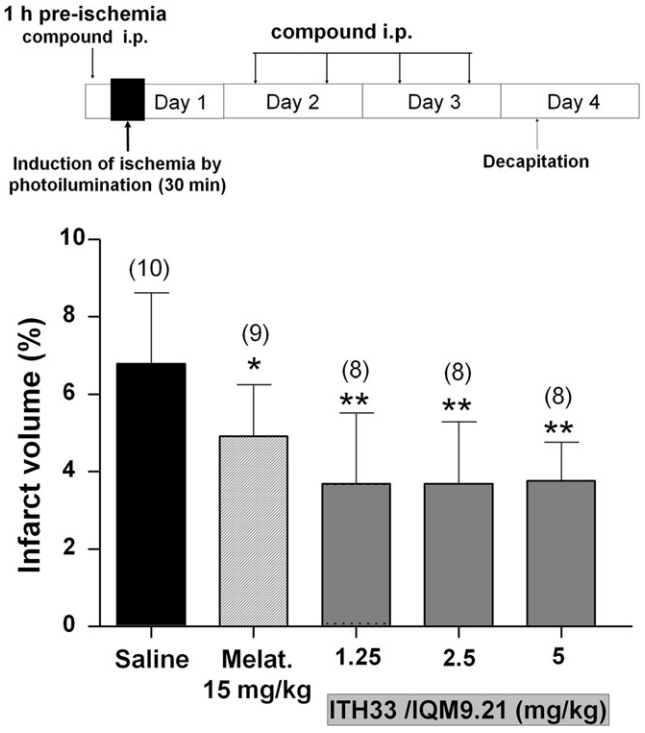

Fig. 6. ITH33/IQM9.21 given before and after photothrombotic focal ischemia induction reduces infarct volume. The top part of the figure illustrates the experimental protocol used. The bottom bar graph represents the averaged data of cerebral infarct volume for each treatment group; control group was treated with saline, melatonin was used as a positive control and ITH33/IQM9.21 was tested at three different doses (1.25, 2.5 and 5 mg/kg). Data correspond to the mean and S.E.M of the number of animals indicated on top of each bar. Statistically significant differences were determined with ANOVA test followed by Bonferroni post hoc. $^{*}p < 0.05$; $^{**}p < 0.01$ compared to saline.

Furthermore, sensorimotor parameters monitored with the "turning in alley" and the "falling from a pole" tests were unchanged in the different animal groups (data not shown).

In control saline-injected animals, the mean volume of cortical infarct was 7%. Used as a positive control, melatonin reduced by 31% the infarct volume. At the lowest dose used (1.25 mg/kg), ITH33/IQM9.21 reduced infarct volume by 47%; higher doses (2.5 and 5 mg/kg) produced similar reductions (Fig. 6). Brain edema was also evaluated in order to correct infarct volume for possible variations of edema. The volume of edema produced by the photothrombotic insult accounted for 3.4 + 2.8% of the total cerebral volume in control animals. Neither melatonin nor ITH33/IQM9.21 caused significant variations of edema.

In order to better mimic the clinical situation of a stroke patient, we used a post-stroke treatment employing the dose of 5 mg/kg (see protocol described in Fig. 7A). When ITH33/IQM9.21 was first administered 1 h post-stroke induction, followed by 2 doses/day the following 2 days, the compound was also able to significantly reduce infarct volume by 50% (Fig. 7B and C).

4. Discussion

In this investigation we describe that the novel MTL compound ITH33/IQM9.21 provides neuroprotection on an *in vitro* model of cerebral ischemia, namely the rat hippocampal slice subjected to OGD/Reox (Fig. 2) as well as on an *in vivo* model of stroke that is, cortical infarct elicited by photothrombosis in the mouse (Figs. 6 and 7). Judging from the results obtained in isolated hippocampal neurons and hippocampal slices, it seems that this compound could afford neuroprotection through a mechanism that implicates reduction of cytosolic calcium overload, mitochondrial protection and antioxidant effects.

Mitigation by ITH33/IQM9.21 of ROS production during OGD/Reox (Fig. 3A–D) is consistent with our previous observation that

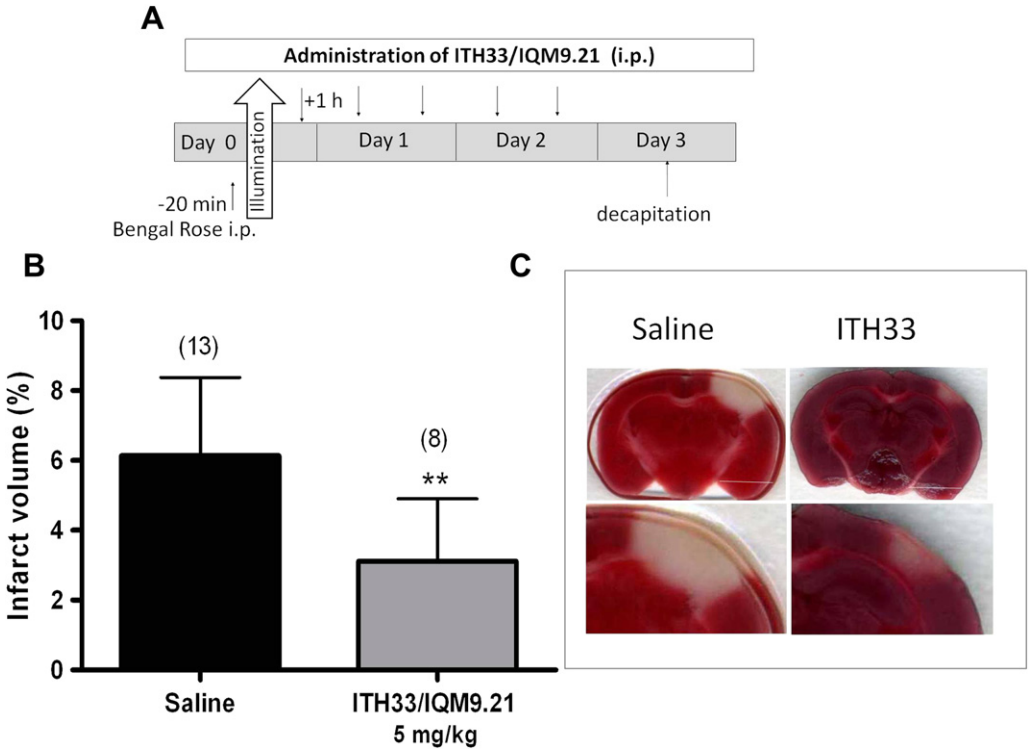

Fig. 7. ITH33/IQM9.21 administered 1-h post-photothrombosis induction reduced cerebral infarct volume. (A) Experimental protocol. (B) Mean infarct volume of mice treated with saline (control) or 5 mg/kg of ITH33/IQM9.21. Data correspond to the mean and SEM of 12 (control) and 8 (ITH33/IQM9.21) animals. (C) Representative images of brain slices stained with TTC of the two experimental groups; the images below show an amplification of the infarct area. Statistically significant differences were determined with ANOVA test followed by Bonferroni post hoc $^{**}p < 0.01$ compared to saline.

this family of compounds protect human neuroblastoma SH–SY5Y cells against the neurotoxic effects of H_2O_2 as well as against exposure to combined oligomycin-A plus rotenone, to augment free radical production through inhibition of the mitochondrial respiratory chain (Arce et al., 2009). It is also consistent with the observation that enhanced iNOS expression under OGD/Reox stress, was interrupted in the presence of ITH33/IQM9.21. The importance of iNOS during brain ischemia is supported by the following observations: (i) excess NO production as a consequence of iNOS induction contributes to brain damage; (ii) the mRNA, the protein and the enzymatic activity of iNOS are increased after transient or permanent brain ischemia in rodents (Grandati et al., 1997; Iadecola et al., 1995a); (iii) iNOS knockout mice present smaller infarcts and better neurological outcomes after middle cerebral artery occlusion, in comparison with their littermates (Iadecola et al., 1995b); and (iv) iNOS inhibitors and NO scavengers are neuroprotective against OGD/Reox models (Cardenas et al., 2000). Therefore, reduction of iNOS, as observed with ITH33/IQM9.21 (Fig. 3F), can be beneficial during a brain ischemic episode.

Continuing with oxidative stress, GSH is the most important low molecular weight antioxidant synthesized in cells; it plays critical roles in protecting cells from oxidative damage and the toxicity of xenobiotic electrophiles, and it maintains the redox homeostasis. We have observed that ITH33/IQM9.21, besides reducing iNOS was able to mitigate GSH depletion occurring OGD/Reox in hippocampal slices (Fig. 4A). The capability of ITH33/IQM9.21 to reduce iNOS induction and prevent GSH depletion indicates that this compound has the ability to protect neurons under oxidative stress conditions as happens to be the case during ischemia-reperfusion.

Another finding that was relevant in the context of neuroprotection, was linked to the prevention by ITH33/IQM9.21 of mitochondrial depolarization occurring during OGD/Reox exposure of hippocampal slices (Fig. 4E). A pH gradient formed when Ca^{2+} is added to energized mitochondria (Saris and Carafoli, 2005) and a burst of respiration occurs (Chance and Williams, 1956). This Ca^{2+} uptake through the uniporter causes $2H^+/1Ca^{2+}$ stoichiometry leading to mitochondrial depolarization (Reynafarje and Lehninger, 1977). Thus, it has been shown that during exposure of rat hippocampal slices to OGD/Reox, an augmentation of the $[Ca^{2+}]_c$ is produced, thereby leading to excess mitochondrial Ca^{2+} uptake, mitochondrial depolarization and the eventual activation of the Ca^{2+}-dependent apoptotic cascade (Zhang and Lipton, 1999). At 3 μM, ITH33/IQM9.21 markedly reduced the mitochondrial membrane potential caused by OGD/Reox (Fig. 4E), in agreement with its ability to block Ca^{2+} entry through NMDA and VDCCs and the ensuing elevations of $[Ca^{2+}]_c$ as observed in the experiments performed in isolated hippocampal neurons (Fig. 5). It is therefore plausible that mitochondrial protection provided by ITH33/IQM9.21 could be linked to its capacity to reduce Ca^{2+} entry and $[Ca^{2+}]_c$ elevations in hippocampal slices subjected to OGD/Reox. These results are in line with those described by Maroto and coworkers that show that ITH33/IQM9.21 blocks voltage-dependent Ca^{2+} channels (VDCCs) in a concentration-dependent manner and also mitigates depolarization-evoked $[Ca^{2+}]_c$ elevations (Maroto et al., 2011).

Although OGD/Reox is widely used as an *in vitro* model of cerebral ischemia, it was important to explore if ITH33/IQM9.21 could also provide neuroprotection on an *in vivo* model; ITH33/IQM9.21 happened to halve the infarct volume elicited by photothrombosis in mice. In this model, the injected Rose Bengal generated oxygen singlets upon illumination of the brain cortex; this causes peroxidation of endothelial cell membranes, occlusive platelet aggregation, microthrombi formation and focal cerebral ischemia (Van Reempts et al., 1987). As previously shown to be the

case in this model (Zou et al., 2006), we also observed that melatonin, used as a positive control, caused a reduction of infarct size. This together with the fact that compound ITH33/IQM9.21 showed antioxidant effects in hippocampal slices stressed with OGD/Reox, suggests that reduction of infarct volume elicited by ITH33/IQM9.21 could be linked, at least, to its antioxidant profile. Worth of note is the observation that at 15 mg/kg, melatonin caused 28% reduction of infarct volume while 1.25 mg/kg of ITH33/IQM9.21 produces 45% reduction, suggesting a higher neuroprotective effect of this compound. We did not observe a dose–response effect of ITH33/IQM9.21 on the reduction of the infarct volume; higher doses of the compound (2.5 and 5 mg/kg) afforded the same effect as 1.25 mg/kg, indicating that this was the maximum effective dose. Furthermore, ITH33/IQM9.21, administered 1 h post-stroke, was also able to maintain its capacity to reduce infarct volume as observed in the pre-administration protocol. In one of the first publications (Watson et al., 1985) of the photochemically induced focal ischemia with bengal rose it is described that the full closure of the vessels occurs as long as 4 h after illumination. This is particularly interesting if we consider that in the present study the first application of ITH33/IQM9.21 was 1 h after ischemia induction as a post-treatment. Hence, the vessels in question were probably not fully closed, which might be allowed the penetration of ITH33/IQM9.21 into the deep layers of penumbra. The fact that the compound was able to protect to a similar extent when administered as pre or post-ischemic treatment suggests that it does not seem to require the induction of proteins, at least in the initial phases, to induce protection, and that it could prevent progression of the penumbra area, an consequently, reduce post-stroke sequelae.

Finally, we would like to make some considerations on the mechanism(s) involved in the neuroprotective effects of ITH33/IQM9.21. Within minutes after an ischemic accident, the core of the brain tissue exposed to the more drastic blood blow reduction undergoes necrotic cell death. This infarct is surrounded by a zone of less severely affected tissue which is rendered functionally silent by reduced blood flow, but still has the capacity for recovery. In this ischemic penumbra many vulnerable neurons may undergo apoptosis after several hours or days (Broughton et al., 2009) thus contributing to infarct expansion (Choi, 1996). In stroke, OGD causes rapid energy depletion, loss of ion gradients, membrane depolarization, opening of VDCCs, enhanced glutamate release and excess Na^+ and Ca^{2+} entry through AMPA receptors, excess Ca^{2+} entry through NMDA receptors as well as through VDCCs, neuronal Ca^{2+} overload and cell death (Dirnagl et al., 1999; Mergenthaler et al., 2004). ITH33/IQM9.21 was able to reduce $[Ca^{2+}]_c$ signals induced by glutamate and a depolarizing solution in hippocampal neurons in this study (Fig. 5) and also to block VDCCs in other studies (Maroto et al., 2011). A second target could be the generation of excess free radical production as suggested by its antioxidant effect (Fig. 3). Finally, a third target could be the brain AChE whose inhibition may enhance ACh available at the vulnerable cortical neurons that are richly innervated by cholinergic nerve terminals. Nicotinic agonists cause neuroprotection in hippocampal slices subjected to OGD/Reox in control mice; such neuroprotection was lost in knockout mice for the α7 subtype of nicotinic receptors for ACh (Egea et al., 2007). Thus inhibiting cortical brain AChE, ITH33/IQM9.21 could provide neuroprotection through augmented nicotinic receptor stimulation by increasing available ACh. This is consistent with the observation that galantamine, another AChE inhibitor with similar potency to ITH33/IQM9.21, also caused a neuroprotection *in vivo* models or cerebral ischemia (Fujiki et al., 2005; Lorrio et al., 2007).

In conclusion, our results show that ITH33/IQM9.21 can afford protection in *in vitro* and *in vivo* models of brain ischemia through a multifaceted mechanism i.e. reducing calcium overload, providing mitochondrial protection and antioxidative actions. Therefore, ITH33/IQM9.21 is a new drug that could be of potential interest in situations where brain perfusion is compromised.

Acknowledgments

This work was supported in part by grants from Spanish Ministry of Economy and Competence Ref. SAF2009-12150 and SAF2012-32223 and the Spanish Ministry of Health (Instituto de Salud Carlos III) RETICS-RD06/0026 to MGL. Consejo Superior de Investigaciones Científicas Ref. PIE-201280E074 to MIRF. It was also supported by the following grants to AGG: Fundación Eugenio Rodríguez Pascual; Fundación CIEN, IS Carlos III; and SAF2010-21795 Ministerio de Economía y Competitividad. Instituto de Salud Carlos III (project CP11/00165 and Miguel Servet contract) and European Commission – Marie Curie Actions FP7 (FP7-People-2012-CIG-322156) to R.L. We also thank the continued support of Fundación Teófilo Hernando.

References

Akasofu, S., Kosasa, T., Kimura, M., Kubota, A., 2003. Protective effect of donepezil in a primary culture of rat cortical neurons exposed to oxygen-glucose deprivation. Eur. J. Pharmacol. 472, 57–63.
Alvarez, A., Opazo, C., Alarcon, R., Garrido, J., Inestrosa, N.C., 1997. Acetylcholinesterase promotes the aggregation of amyloid-beta-peptide fragments by forming a complex with the growing fibrils. J. Mol. Biol. 272, 348–361.
Aoyama, K., Watabe, M., Nakaki, T., 2008. Regulation of neuronal glutathione synthesis. J. Pharmacol. Sci. 108, 227–238.
Arce, M.P., Rodriguez-Franco, M.I., Gonzalez-Munoz, G.C., Perez, C., Lopez, B., Villarroya, M., Lopez, M.G., Garcia, A.G., Conde, S., 2009. Neuroprotective and cholinergic properties of multifunctional glutamic acid derivatives for the treatment of Alzheimer's disease. J. Med. Chem. 52, 7249–7257.
Arias, E., Gallego-Sandin, S., Villarroya, M., Garcia, A.G., Lopez, M.G., 2005. Unequal neuroprotection afforded by the acetylcholinesterase inhibitors galantamine, donepezil, and rivastigmine in SH-SY5Y neuroblastoma cells: role of nicotinic receptors. J. Pharmacol. Exp. Ther. 315, 1346–1353.
Broughton, B.R., Reutens, D.C., Sobey, C.G., 2009. Apoptotic mechanisms after cerebral ischemia. Stroke 40, e331–e339.
Brown, G.C., 2010. Nitric oxide and neuronal death. Nitric Oxide 23, 153–165.
Cardenas, A., Hurtado, O., Leza, J.C., Lorenzo, P., Bartrons, R., Lizasoain, I., Moro, M.A., 2000. Fructose-1,6-bisphosphate inhibits the expression of inducible nitric oxide synthase caused by oxygen-glucose deprivation through the inhibition of glutamate release in rat forebrain slices. Naunyn Schmiedebergs Arch. Pharmacol. 362, 208–212.
Crack, P.J., Taylor, J.M., 2005. Reactive oxygen species and the modulation of stroke. Free Radic. Biol. Med. 38, 1433–1444.
Chance, B., Williams, G.R., 1956. The respiratory chain and oxidative phosphorylation. Adv. Enzymol. Relat. Subj. Biochem. 17, 65–134.
Choi, D.W., 1985. Glutamate neurotoxicity in cortical cell culture is calcium dependent. Neurosci. Lett. 58, 293–297.
Choi, D.W., 1996. Ischemia-induced neuronal apoptosis. Curr. Opin. Neurobiol. 6, 667–672.
Denizot, F., Lang, R., 1986. Rapid colorimetric assay for cell growth and survival. Modifications to the tetrazolium dye procedure giving improved sensitivity and reliability. J. Immunol. Methods 89, 271–277.
Dirnagl, U., Iadecola, C., Moskowitz, M.A., 1999. Pathobiology of ischaemic stroke: an integrated view. Trends Neurosci. 22, 391–397.
Egea, J., Rosa, A.O., Sobrado, M., Gandia, L., Lopez, M.G., Garcia, A.G., 2007. Neuroprotection afforded by nicotine against oxygen and glucose deprivation in hippocampal slices is lost in alpha7 nicotinic receptor knockout mice. Neuroscience 145, 866–872.
Ehrenberg, B., Montana, V., Wei, M.D., Wuskell, J.P., Loew, L.M., 1988. Membrane potential can be determined in individual cells from the nernstian distribution of cationic dyes. Biophys. J. 53, 785–794.
Fernandez-Checa, J.C., Kaplowitz, N., 1990. The use of monochlorobimane to determine hepatic GSH levels and synthesis. Anal. Biochem. 190, 212–219.
Fisher, M., Albers, G.W., Donnan, G.A., Furlan, A.J., Grotta, J.C., Kidwell, C.S., Sacco, R.L., Wechsler, L.R., 2005. Enhancing the development and approval of acute stroke therapies: stroke Therapy Academic Industry roundtable. Stroke 36, 1808–1813.
Fujiki, M., Kobayashi, H., Uchida, S., Inoue, R., Ishii, K., 2005. Neuroprotective effect of donepezil, a nicotinic acetylcholine-receptor activator, on cerebral infarction in rats. Brain Res. 1043, 236–241.
Garcia-Alloza, M., Gregory, J., Kuchibhotla, K.V., Fine, S., Wei, Y., Ayata, C., Frosch, M.P., Greenberg, S.M., Bacskai, B.J., 2011. Cerebrovascular lesions induce transient beta-amyloid deposition. Brain 134, 3697–3707.

Gordon-Krajcer, W., Kozniewska, E., Lazarewicz, J.W., Ksiezak-Reding, H., 2007. Differential changes in phosphorylation of tau at PHF-1 and 12E8 epitopes during brain ischemia and reperfusion in gerbils. Neurochem. Res. 32, 729–737.

Grandati, M., Verrecchia, C., Revaud, M.L., Allix, M., Boulu, R.G., Plotkine, M., 1997. Calcium-independent NO-synthase activity and nitrites/nitrates production in transient focal cerebral ischaemia in mice. Br. J. Pharmacol. 122, 625–630.

Ha, H.C., Woster, P.M., Yager, J.D., Casero Jr., R.A., 1997. The role of polyamine catabolism in polyamine analogue-induced programmed cell death. Proc. Natl. Acad. Sci. U.S.A. 94, 11557–11562.

Iadecola, C., Xu, X., Zhang, F., el-Fakahany, E.E., Ross, M.E., 1995a. Marked induction of calcium-independent nitric oxide synthase activity after focal cerebral ischemia. J. Cereb. Blood Flow Metab. 15, 52–59.

Iadecola, C., Zhang, F., Xu, X., 1995b. Inhibition of inducible nitric oxide synthase ameliorates cerebral ischemic damage. Am. J. Physiol. 268, R286–R292.

Iijima, T., 2006. Mitochondrial membrane potential and ischemic neuronal death. Neurosci. Res. 55, 234–243.

Kamencic, H., Lyon, A., Paterson, P.G., Juurlink, B.H., 2000. Monochlorobimane fluorometric method to measure tissue glutathione. Anal. Biochem. 286, 35–37.

Lees, K.R., Zivin, J.A., Ashwood, T., Davalos, A., Davis, S.M., Diener, H.C., Grotta, J., Lyden, P., Shuaib, A., Hardemark, H.G., Wasiewski, W.W., 2006. NXY-059 for acute ischemic stroke. N. Engl. J. Med. 354, 588–600.

Leon, R., Garcia, A.G., Marco-Contelles, J., 2013. Recent advances in the multitarget-directed ligands approach for the treatment of Alzheimer's disease. Med. Res. Rev. 33, 139–189.

Lorrio, S., Sobrado, M., Arias, E., Roda, J.M., Garcia, A.G., Lopez, M.G., 2007. Galantamine postischemia provides neuroprotection and memory recovery against transient global cerebral ischemia in gerbils. J. Pharmacol. Exp. Ther. 322, 591–599.

Mander, P., Borutaite, V., Moncada, S., Brown, G.C., 2005. Nitric oxide from inflammatory-activated glia synergizes with hypoxia to induce neuronal death. J. Neurosci. Res. 79, 208–215.

Maroto, M., de Diego, A.M., Albinana, E., Fernandez-Morales, J.C., Caricati-Neto, A., Jurkiewicz, A., Yanez, M., Rodriguez-Franco, M.I., Conde, S., Arce, M.P., Hernandez-Guijo, J.M., Garcia, A.G., 2011. Multi-target novel neuroprotective compound ITH33/IQM9.21 inhibits calcium entry, calcium signals and exocytosis. Cell Calcium 50, 359–369.

Mergenthaler, P., Dirnagl, U., Meisel, A., 2004. Pathophysiology of stroke: lessons from animal models. Metab. Brain Dis. 19, 151–167.

Moro, M.A., Cardenas, A., Hurtado, O., Leza, J.C., Lizasoain, I., 2004. Role of nitric oxide after brain ischaemia. Cell Calcium 36, 265–275.

Randall, R.D., Thayer, S.A., 1992. Glutamate-induced calcium transient triggers delayed calcium overload and neurotoxicity in rat hippocampal neurons. J. Neurosci. 12, 1882–1895.

Reynafarje, B., Lehninger, A.L., 1977. Electric charge stoichiometry of calcium translocation in mitochondria. Biochem. Biophys. Res. Commun. 77, 1273–1279.

Saris, N.E., Carafoli, E., 2005. A historical review of cellular calcium handling, with emphasis on mitochondria. Biochemistry (Mosc.) 70, 187–194.

Shuaib, A., Lees, K.R., Lyden, P., Grotta, J., Davalos, A., Davis, S.M., Diener, H.C., Ashwood, T., Wasiewski, W.W., Emeribe, U., 2007. NXY-059 for the treatment of acute ischemic stroke. N. Engl. J. Med. 357, 562–571.

Sobrado, M., Roda, J.M., Lopez, M.G., Egea, J., Garcia, A.G., 2004. Galantamine and memantine produce different degrees of neuroprotection in rat hippocampal slices subjected to oxygen-glucose deprivation. Neurosci. Lett. 365, 132–136.

Takada-Takatori, Y., Kume, T., Sugimoto, M., Katsuki, H., Sugimoto, H., Akaike, A., 2006. Acetylcholinesterase inhibitors used in treatment of Alzheimer's disease prevent glutamate neurotoxicity via nicotinic acetylcholine receptors and phosphatidylinositol 3-kinase cascade. Neuropharmacology 51, 474–486.

Van Reempts, J., Van Deuren, B., Van de Ven, M., Cornelissen, F., Borgers, M., 1987. Flunarizine reduces cerebral infarct size after photochemically induced thrombosis in spontaneously hypertensive rats. Stroke 18, 1113–1119.

Watson, B.D., Dietrich, W.D., Busto, R., Wachtel, M.S., Ginsberg, M.D., 1985. Induction of reproducible brain infarction by photochemically initiated thrombosis. Ann. Neurol. 17 (5), 497–504.

Zhang, Y., Lipton, P., 1999. Cytosolic Ca2+ changes during in vitro ischemia in rat hippocampal slices: major roles for glutamate and Na+-dependent Ca2+ release from mitochondria. J. Neurosci. 19, 3307–3315.

Zou, L.Y., Cheung, R.T., Liu, S., Li, G., Huang, L., 2006. Melatonin reduces infarction volume in a photothrombotic stroke model in the wild-type but not cyclooxygenase-1-gene knockout mice. J. Pineal Res. 41, 150–156.